Case Studies in Construction Materials 17 (2022) e01218

Contents lists available at ScienceDirect

Case Studies in Construction Materials

journal homepage: www.elsevier.com/locate/cscm

Degradation of concrete in marine environment under coupled chloride and sulfate attack: A numerical and experimental study

Dandan Sun [a,b], Zhenjie Cao [b], Changfu Huang [b], Kai Wu [a,*], Geert De Schutter [c], Lihai Zhang [d]

[a] Key Laboratory of Advanced Civil Engineering Materials of Ministry of Education, School of Materials Science and Engineering, Tongji University, Shanghai 201804, China
[b] Technology Center, China Railway 15 Bureau Group CO., LTD., Shanghai 200040, China
[c] Magnel Laboratory for Concrete Research, Ghent University, Ghent 9052, Belgium
[d] Department of Infrastructure Engineering, The University of Melbourne, Melbourne, VIC 3010, Australia

ARTICLE INFO

Keywords:
Offshore concrete structure
Chloride ions
Sulfate ions
Competitive binding
Reactive-transport

ABSTRACT

The corrosion of offshore reinforced concrete structures under combined chloride and sulfate ions attack is a complex corrosion phenomenon. The purpose of this study is to develop numerical models in conjunction with experimental studies for long-term durability assessment of offshore concrete structures. A numerical model was developed to describe the simultaneously transport of chloride and sulfate ions considering the competitive binding by hardened cement pastes effect. The model was validated by a series of experimental studies. The validated model was implemented to predict the service life of the offshore RC structures under various chloride and sulfate solutions. The results show that chloride ions induced corrosion of steel bars in offshore RC structures is highly influenced by the concentration of sulfate ions. The sulfate ions induced concrete expansion and cracking from ettringite formation could potentially accelerate chloride ions induced corrosion of steel bars in concrete, ultimately the premature failure of the offshore RC structures.

1. Introduction

Under aggressive marine environment, the offshore reinforced concrete (Delagrave, Marchand et al.) structures are vulnerable to the attack of various harmful ions like sulfate ions, chloride ions and magnesium ions [1,2]. Sulfate attack on concrete leads to the generation of degradation products, such as gypsum and tricalcium sulfoaluminate hydrate (ettringite), which could result in expansion, cracking, loss of strength and ultimately failure of concrete structure [3,4]. In addition, the chloride-induced reinforcement corrosion can also significantly influence the durability of concrete structures [5,6]. Chloride ions normally exist in pore solution in the form of free ions or be bound by the hydrated product which could slow down the ingress of chlorides [7-9]. Both sulfate and chloride ions are harmful for the service life of offshore concrete structures. However, the studies on understanding the combined attack mechanism of sulfate and chloride ions are still limited so far.

As shown in Fig. 1, under marine environmental condition, the majority of harmful ions in seawater are chloride and sulfate ions [10]. The joint attack of chloride, sulfate and other ions may lead to a synergetic damage to the offshore structures [11,12], and the

* Corresponding author.
E-mail addresses: wukai@tongji.edu.cn, sddmaterial@foxmail.com (K. Wu).

https://doi.org/10.1016/j.cscm.2022.e01218
Received 5 April 2022; Received in revised form 29 May 2022; Accepted 1 June 2022
Available online 6 June 2022

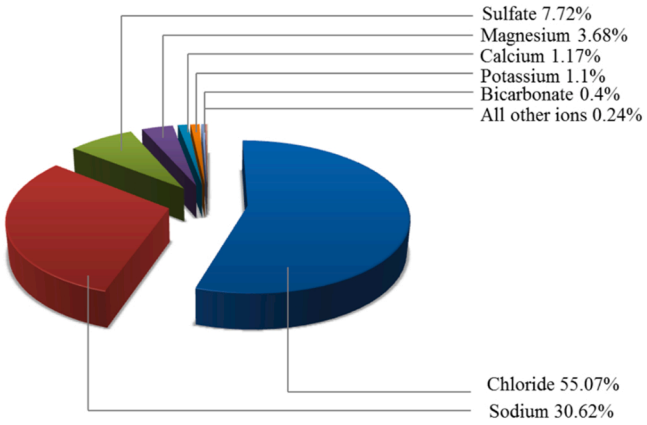

Fig. 1. Composition of seawater (Data from [16]).

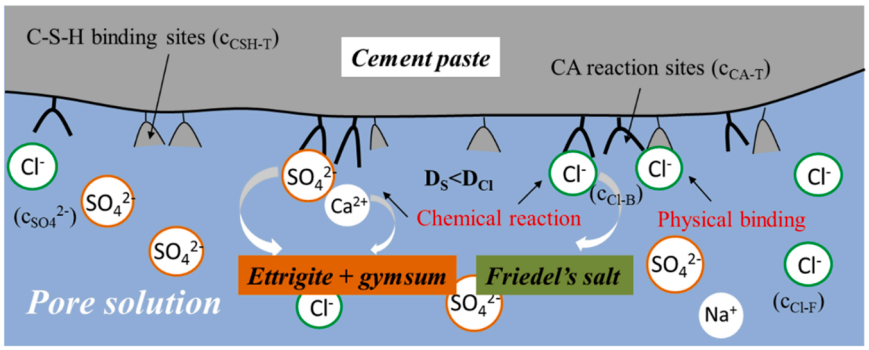

Fig. 2. Schematic diagram of the interaction between penetrated ions and hardened cement pastes.

research outcomes in this area are still controversial. For example, Sotiriadis et al. [13] pointed out that the chloride ions show a positive effect by delaying the transport of sulfate ions and mitigating the so caused deterioration [13], whereas Abdalkader et al. (2013) found that sulfate caused degradation is more serious when specimens were immersed in the combined sulfate and chloride solution (Abdalkader, Lynsdale et al., 2013). Maes et al. (2014) observed that sulfate ions enhance the transport performance of free chlorides into the concrete specimens during a relatively short period of time (*e.g.* 7–14 weeks) [14]. In contrast, Zhang et al. [15] indicated that the penetration of ions could be delayed at early stage due to the filling of pores [15].

Chlorides and sulfates penetrate into concrete by means of capillary suction and diffusion, so diffusivity is the transport mechanism determining penetration and attack of ions [17,18]. At early stage, the accumulation of reaction products (*i.e.* gypsum, ettringite and Friedel's salt, etc) could decrease the available pore volume of concrete and thereby inhibits the transport of ions into the concrete [14, 19]. The increase of ettringite formation gradually accelerates the expansion of concrete with time, ultimately leads to a more serious cracking and chloride-induced corrosion of reinforcement bars in concrete [20,21]. Furthermore, there is a competitive binding between chlorides and sulfate ions with the CA binding sites (*i.e.* hydrated and unhydrated calcium aluminate)[22,23]. K Rimvydas found that chloride ions penetrate into concrete and react with monosulfoaluminate to form Friedel's salt, which could release sulfate ions by reducing the formation of ettringite [23]. Due to the combination of chloride ions by aluminate phases in concrete, more sulfate ions is able to transport into the concrete furtherly.The competitive relation between chloride and sulfate ions is also influenced by temperature and Ca^{2+} which facilitated the stabilized the C-S-H phase [24,25].

To date, the competitive binding of sulfate and chloride ions in concrete and its effects on corrosion of steel bars in concrete have not been fully understood and relevant studies in this field are still limited. Therefore, this study aims to develop a systematic model for investigating the durability of concrete under the attack of various combinations of chloride and sulfate concentrations. The model was proposed to describe the ions transport, competitive reaction and micro-mechanical behavior, and was calibrated by a series of experimental data.

2. Methodology

The reactive transportation of combined sulfate and chloride ions contains a series of complicated processes. In this study, the processes were simplified as shown in Fig. 2 based on previous literature research [26,27,14,28,29]. Due to the relatively high diffusion coefficient and concentration gradient of chloride ions in comparison to sulfate ions [30], chloride ions firstly penetrate into

concrete to form Friedel's salt by reacting with calcium aluminate (CA) or physically binding with the hydrated compounds. Later on, the formation of reaction product induced by sulfate ions could leads to a variation of pore structure and even swelling and cracking in concrete [15,31], which further enhances the transport of chloride ions. The definitions of C-S-H binding site and CA reaction site were proposed in this study to describe the chemical reaction and physical binding of ions with the hydrated system quantitatively.

2.1. Governing equations

The governing equations to describe the transport and competitive binding of chloride and sulfate ions in concrete are based on the porous media theory [32,33]. The total ions concentrations consist of free ions and the ions attached to the hydrated cement physically and chemically. That is,

$$\overline{c}_j = \overline{c}_j^f + \sum_{i=1}^{2} \overline{c}_{ji}^s, \mathrm{j} = 1, \quad 2 \tag{1}$$

in which

$$\overline{c}_j = \phi^f \cdot c_j \tag{2}$$

where $i = 1$ refers to C-S-H, $i = 2$ refers to hydrated calcium aluminate composite (CA), $j = 1$ refers to Cl^- and $j = 2$ refers to SO_4^{2-}. $\overline{c}_j$ and c_j represents the matrix-based and fluid-based ion concentration, respectively. $\overline{c}_j^f$ and $\overline{c}_j^s$ represents the matrix-based free and fixed ion concentration, respectively. ϕ^f represents volume fraction of fluid phase in porous media, which is assumed to be the porosity when the concrete specimen is in saturated state. It is worth to mention that the contribution of C-S-H to SO_4^{2-} was ignored due to their low binding affinity (*i.e.* $\overline{c}_{21}^s = 0$).

2.2. Conservation of mass

When chloride and sulfate ions transport into concrete, mass conversion occurs due to a series of reactions or binding processes. The conservation of mass could be expressed as:

$$\frac{\partial\left(\phi^f c_j^f\right)}{\partial t} + \nabla \cdot \left(-\phi^f D_j \nabla c_j^f\right) = -\sum\nolimits_{i=1}^{2} S_{ji}, \mathrm{j} = 1, \tag{3}$$

where S_{ji} is source sink term. D_j represents the diffusion coefficient of chloride or sulfate ions and can be determined using the reverse Hill Function which describes the decrease of D_j resulting from the fill effect of ettringite and Friedel's salt in the pores. That is,

$$D_j = D_j^0 \left(\frac{1}{1 + \left(\frac{V_{AFt}}{K_{a1} V_p^{max}}\right)^{m_1}} \right) \left(\frac{1}{1 + \left(\frac{V_{Frie}}{K_{a2} V_p^{max}}\right)^{m_2}} \right), \mathrm{j} = 1, \quad 2 \tag{4}$$

in which,

$$D_j^0 = D_j^{water} \varphi \tau = 2\varphi D_j^{water} \Big/ (3 - \varphi) \tag{5}$$

where D_j^0 and D_j^{water} is the initial ion diffusion coefficient in concrete and water, respectively. V_{AFt}/V_p^{max} and V_{Frie}/V_p^{max} is the ratio of the ettringite and Friedel's salt volume to the maximum fillable pore volume. K_{a1} and K_{a2} is activation factor describing the values of V_{AFt}/V_p^{max} and V_{Frie}/V_p^{max} which result in a significant decrease of D_j. m_1 and m_2 represents the steepness of Hill-equation, φ is the porosity of concrete (*i.e.* ϕ^f) and τ represents the tortuosity of the pore system in porous media.

The theoretical volume of the ettringite and Friedel's salt (V_{AFt} and V_{Frie} in Eq. (4)) can be defined as [34],

$$V_k = c_k \phi^f N_A r_k, \mathrm{k} = 1, 2 \tag{6}$$

where $k = 1$ refers to ettringite, $k = 2$ refers to Friedel's salt, c_k is the concentration of ions, N_A represents Avogadro constant and r_k represents the estimated molecular volume of reaction product k, *i.e.* ettringite and Friedel's salt.

2.3. The law of mass action

It is well known that chloride and sulfate ions transport into the porous concrete structures with ion dissipation. During the transport process, chemical reactions among sulfates, portlandite (CH), hydrated and unreacted aluminates lead to the formation of gypsum and ettringite [35]. In addition, chlorides can bind on the surface of pores (mostly on C-S-H and other hydrated cement phase) or react with CA to form the so-called Friedel's salt [36,37]. The chemical reactions can be described as,

$$Sulfate\ ion\ SO42-:\ Ca^{2+}+SO_4^{2-}+2H\rightarrow C\overline{S}H_2\quad(gypsum) \tag{7}$$

$$\left\{\begin{array}{c} C_3A+C\overline{S}H_2+26H\rightarrow C_6A\overline{S}_3H_{32}(ettringite)\\ C_4AH_{13}+3C\overline{S}H_2+14H\rightarrow C_6A\overline{S}_3H_{32}(ettringite)+CH\\ C_4A\overline{S}H_{12}+2C\overline{S}H_2+16H\rightarrow C_6A\overline{S}_3H_{32}(ettringite)\\ 3C_4AF+12C\overline{S}H_2+aH\rightarrow 4C_6A\overline{S}_3H_{32}\quad(ettringite)+2[(A,F)H_3] \end{array}\right\} \tag{8}$$

$$Chloride\quad ion\quad Cl-:\ Ca^{2+}+2Cl^{-}+C_3A+10H\rightarrow C_3A{\cdot}CaCl_2\cdot 10H_2O\quad(Friedel's\quad salt) \tag{9}$$

Eqs. (7–9) can be further simplified as follows,

$$solute_j+B_i\underset{k_{-ji}}{\overset{k_{+ji}}{\rightleftharpoons}}complex_{ji},\mathrm{j}=1,\quad 2;\ \mathrm{i}=1,\quad 2 \tag{10}$$

where $solute_j$ represents Cl^- and SO_4^{2-}; B_i represents binding sites on pore surface, such as CA and C-S-H, *etc.* k_{+ji} and k_{-ji} are associations and dissociation rate constants, respectively, which can be obtained from previous research [38,34,39] and $complex_{ji}$ represents the reaction (binding) products. It should be noted that if the reaction is non-reversible, k_{-ji} in Eq. (10) equals to 0. The detailed law of mass action of each component can be expressed as,

$$Free\ chloride\ ion\ Cl-:\frac{\partial\left(\phi_f c_{Cl-F}\right)}{\partial t}=-k_{11}\phi_f c_{Cl-F}\left(1-\phi_f\right)c_{CSH-T}+k_{-11}\left(1-\phi_f\right)c_{Cl-B}-k_{12}\phi_f c_{Cl-F}\left(1-\phi_f\right)c_{CA} \tag{11}$$

$$Sulfate\ ion\ SO42-:\frac{\partial_{cSO_4^{2-}}}{\partial t}=-k_{22}\cdot c_{Ca^{2+}}\cdot c_{SO_4^{2-}}\cdot\left(c_{CA}\right)^{1/n} \tag{12}$$

$$CA\ \ binding\ site:\frac{\partial c_{CA}}{\partial t}=-k_{22}\cdot c_{Ca^{2+}}\cdot c_{SO_4^{2-}}\cdot\left(c_{CA}\right)^{1/n}-k_{12}\phi_f C_F\left(1-\phi_f\right)c_{CA} \tag{13}$$

$$Ettringite:\frac{\partial c_{Ett}}{\partial t}=k_{22}\cdot c_{Ca^{2+}}\cdot c_{SO_4^{2-}}\cdot\left(c_{CA}\right)^{1/n} \tag{14}$$

$$Friedel's\quad salt:\frac{\partial\left[\left(1-\phi_f\right)c_{Frie}\right]}{\partial t}=k_{12}\phi_f c_{Cl-F}\left(1-\phi_f\right)c_{CA} \tag{15}$$

where $c_{CSH\text{-}T}$ and c_{CA} is the theoretical concentration of hydrated cement (mainly C-S-H) and calcium aluminate phases, which provides available binding sites for both Cl^- and SO_4^{2-}. c_{Ett} and c_{Frie} is the concentration of ettringite and Friedel's salt, respectively.

2.4. Constitutive equation

The accumulation of ettringite causes the overall expansion of concrete and the propagation of micro and macro-cracks associated with progressive reduction of stiffness and strength. In order to obtain the crack initiation time caused by the expansion of deterioration products (*i.e.* ettringite), the constitutive equations considering inner crystal pressure was used [34]. Assuming the total stress in concrete is the sum of internal pressure caused by ettringite and the elastic stress of paste, the governing equation can be defined as,

$$\nabla\boldsymbol{\sigma}+\boldsymbol{F_{Ett}}=\boldsymbol{C}:\varepsilon_e+\boldsymbol{F_{Ett}}=\rho\frac{\partial^2\boldsymbol{u}}{\partial t^2} \tag{16}$$

where $\boldsymbol{\sigma}$ is Cauchy stress tensor, $\boldsymbol{F_{Ett}}$ represents the isotropic internal stress in a RVE (Representative volume element) of cement paste, ε_e represents the strain tensor caused by the stress acting on the pore surface and $\boldsymbol{u}$ represents the following displacement vector. The isotropic internal stress $\boldsymbol{F_{Ett}}$ caused by ettringite expansion can be described as [34],

$$F_{Ett}=\frac{V_{max}\left(c_{Ett}/c_{Ett\_max}\right)^{\omega}}{K^{\omega}+\left(c_{Ett}/c_{Ett\_max}\right)^{\omega}} \tag{17}$$

where V_{max} represents ettringite-induced maximum internal stress; K is activation coefficient representing the significant increase of F_{Ett} when c_{Ett} reaches to a certain threshold. ω is steepness of the curve ranging from 1 to 6.

2.5. Initial and boundary conditions

Eq. (18) and Eq. (19) expresses the initial and boundary conditions for this numerical model, and the concentrations can be expressed in terms of RVE.

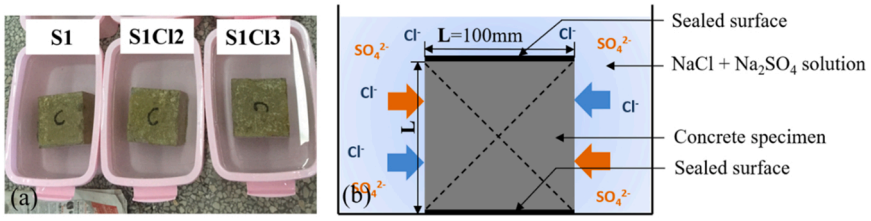

Fig. 3. Procedure of ion diffusion test. (a) experimental procedure, and (b) schematic diagram of immersion experimental procedure.

Table 1
The parameters used in the reactive transport model of sulfate and chloride ions.

Parameter	Value	Reference
c_{Ca2+}	21.25 (mol/m^3)	Nakarai et al., ($year$) [40]
$c_{CA\text{-}T}$	117.06 (mol/m^3)	Obtained in experimental study
D_1^{water}	2.032×10^{-9} (m^2/s)	Lide ($year$) [30]
D_2^{water}	1.07×10^{-9} (m^3/s)	Gospodinov et al., ($year$) [41]
k_{11}	1×10^{-8} (m^3/mol·s)	Papadakis et al., ($year$) [42]
k_a	1.3×10^{-2} (m^3/mol)	Papadakis et al., ($year$) [42]
k_{12}	1.21×10^{-10} (m^3/mol·s)	Suryavanshi et al., ($year$) [43,44]
k_{22}	1.9×10^{-10} (m^3/mol·s)	Sun et al., ($year$) [34,45]
K	0.2	Sun et al., ($year$) [34]
ω	2	Sun et al., ($year$) [34]

Table 2
Concrete mixture prepared for the experiment.

	OPC	Sand 0/5 mm	Aggregate 5/8 mm	Aggregate 8/10 mm	Water
Content (kg/m^3)	833	1173.3	318	1098	380

Table 3
The compositions of corrosive solutions.

	Solution	mass content in the solution
S1	35.2 mol/m^3 Na_2SO_4	0.5% Na_2SO_4
S1Cl2	35.2 mol/m^3 Na_2SO_4 + 70.4 mol/m^3 NaCl	0.5% Na_2SO_4 + 0.4% NaCl
S1Cl3	35.2 mol/m^3 Na_2SO_4 + 105.6 mol/m^3 NaCl	0.5% Na_2SO_4 + 0.8% NaCl

$$\left\{\begin{array}{c} c_s(x,t=0)=0, \\ c_c(x,t=0)=0, \\ c_{CA}(x,t=0)=c_{CA-T}, \\ c_{Ett}(x,t=0)=0, \end{array}\right\} \tag{18}$$

$$\left\{\begin{array}{ll} c_{SO_4^{2-}}(x=0,t)=\phi_f c_{s0}, & c_{SO_4^{2-}}(x=L,t)=\phi_f c_{s0} \\ c_{Cl-F}(x=0,t)=\phi_f c_{c0}, & c_{Cl-F}(x=L,t)=\phi_f c_{c0} \\ c_{CA}(x=0,t)=c_{CA-T}, & c_{CA}(x=L,t)=c_{CA-T} \\ c_{Ett}(x=0,t)=0, & c_{Ett}(x=L,t)=0 \end{array}\right\} \tag{19}$$

where x and t represents the section position and immersion time of concrete specimen, respectively. L is 100 mm as shown in Fig. 3; c_{CA-T} is the initial concentration of CA. c_{s0} and c_{c0} is the concentration of sulfate ions and chloride ions in solution, respectively.

The parameters used to describe the ion transport, chemical and mechanical behavior of concrete are shown in Table 1.

3. Experimental program

3.1. Materials and specimen preparation

The cement used in experimental study is ordinary Portland cement (OPC 52.5 R), and the mixture of the designed specimen is given in Table 2. Cubes (100 × 100 × 100 mm^3) were cast with a water to cement ratio (W/C) of 0.45. Specimens were demoulded

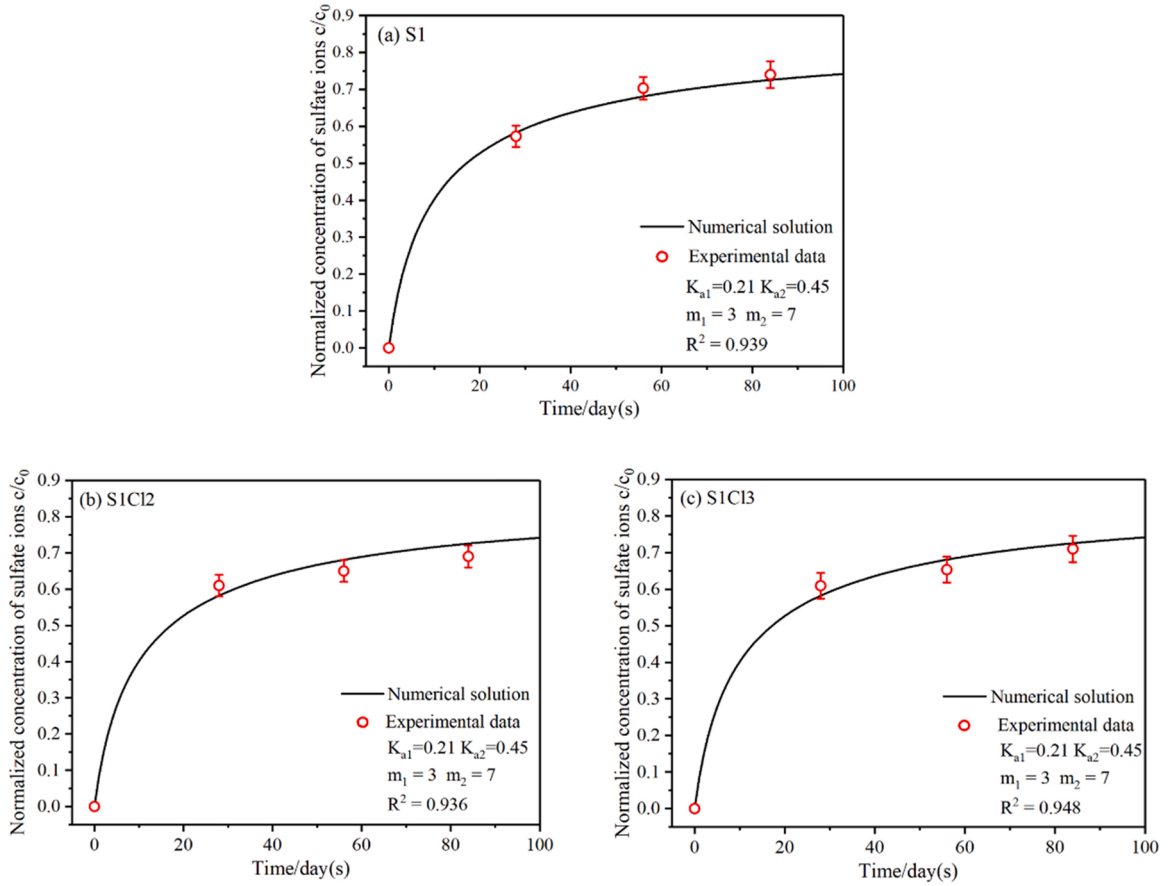

Fig. 4. Normalized concentration of sulfate ions with time when specimens were immersed in (a) 35.2 mol/L Na_2SO_4, (b) 35.2 mol/L Na_2SO_4 + 70.4 mol/L NaCl, and (c) 35.2 mol/L Na_2SO_4 + 105.6 mol/L NaCl solution.

after 24 h and cured in the chamber with a relative humidity of 95 ± 5% and temperature of 20 ± 2 ℃ for 56 days.

3.2. Diffusion test

Specimens were immersed in three different test solutions after 56 days of curing as shown in Table 3. Type A contained 0.5% Na_2SO_4 solution, Type B and Type C contained 0.5% Na_2SO_4 combined with 0.4% and 0.8% NaCl solution was prepared respectively. The corrosive solutions were replaced every month to maintain a stable ion concentration.

Four sides of the specimens were sealed by epoxy resin after 56 days of initial curing and then transferred into the corrosive solution. The final results were obtained from 3 specimens to obtain average values. The experiments conducted in this study follow the Barium Sulfate Gravimetric method (GB/T 22660.8–2008). The powder of 0–5 mm layer on the surface of the specimens was obtained by drilling every 4 weeks and dissolved 0.5 g in 100 mL water after being dried to a constant weight. Heated $BaCl_2.2\ H_2O$ was used to form $BaSO_4$ solid with SO_4^{2-}, and the content of sulfate could then be estimated after filtration and high temperature calcination.

The mass content of SO_4^{2-} can be expressed as:

$$w\left(SO_4^{2-}\right) = \frac{0.4116 \times (m_2 - m_1)}{m_0} \times 100 \tag{20}$$

where 0.4116 is the coefficient of conversion of $BaSO_4$ to SO_4^{2-}; m_2 and m_1 represents the mass of $BaSO_4$ in the test sample and blank sample, and m_0 is the mass of test sample.

4. Results and discussion

4.1. Comparison with experimental study

Fig. 4 reveals that the transport of sulfate ions under different corrosive solution can be modelled by using one set of parameters in Eq. (4) (*i.e.* $K_{a1} = 0.21$, $K_{a2} = 0.45$, $m_1 = 2$ and $m_2 = 7$) which describe the decrease of diffusion coefficients considering the filling

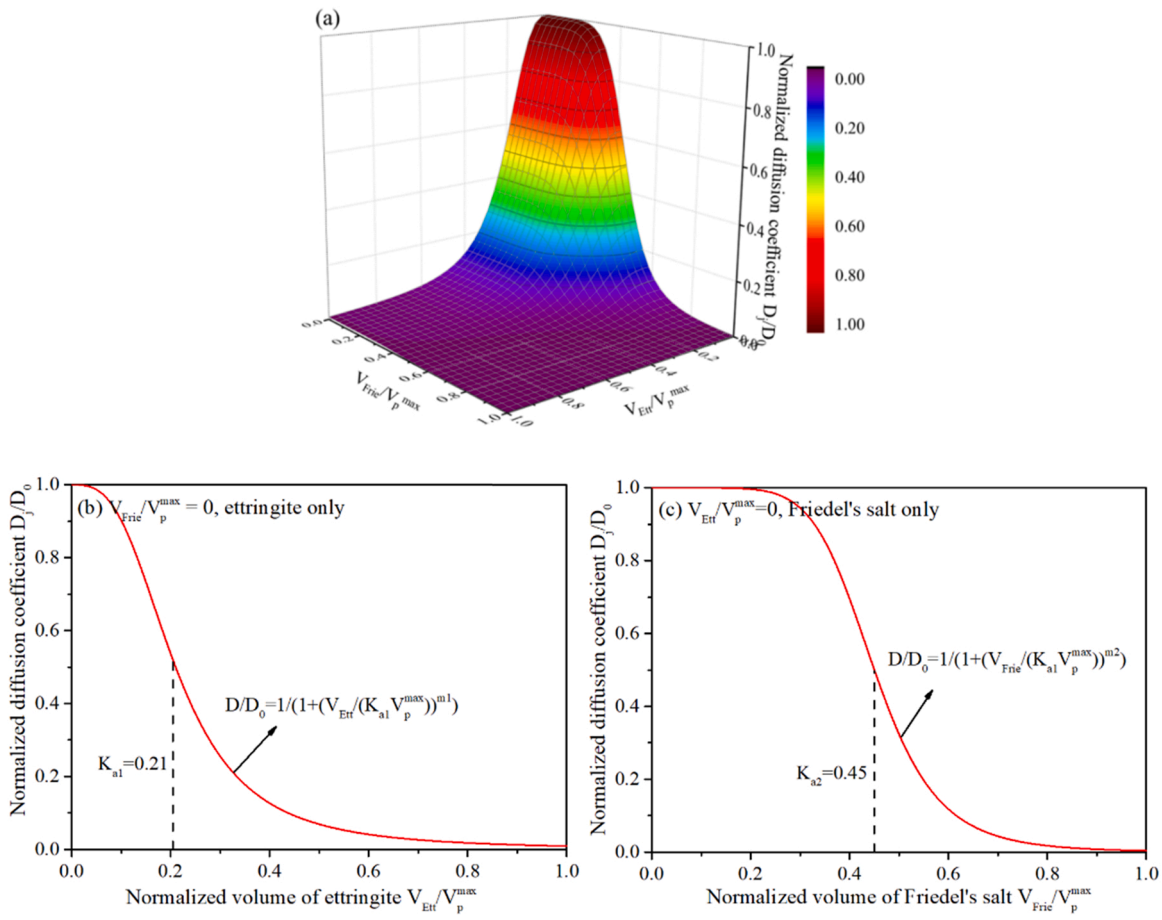

Fig. 5. Normalized diffusion coefficient of ions ($j = 1$ refers to Cl^- and $j = 2$ refers to SO_4^{2-}) caused by filling effect under (a) various combination of ettringite and Friedel's salt contents, (b) ettringite only (V_{Frie}/V_p^{max}) and (c) Friedel's salt only (V_{Ett}/V_p^{max}).

effects of reaction products in the pores before cracks generation. The numerical simulation results in Fig. 4(a)-(c) show similar trends and the sulfate concentration increases significantly during the first 20 days of immersion and then slows down gradually. Concentration gradient between environmental condition and pore solution is considered to be the main reason for the significant increase during early stage. The results also show that experimental data and the numerical solution fit well with one set of parameters, but the interaction between different ions and its influence on ion transport need to be further discussed.

4.2. Diffusion coefficient of ions

Early stage penetration before cracking is mainly focused in this study. The presence of sulfate ions influences the transport of chloride ions and then the degradation of concrete remarkable. For example, the filling of reaction products leads to the refining of pore structure and consequently mitigates the risk of chloride initiated corrosion [14]. Fig. 5 shows the change of diffusion coefficient considering the filling effect caused by both ettringite and Friedel's salt when concrete structures are immersed in a mixture of chloride and sulfate solution. As shown in Eq. (4), K_{a1} and K_{a2} represents the activation coefficient of ettringite and Friedel's salt, respectively. It can be seen from Fig. 5(b) and (c) that a significant decrease of the normalized diffusion coefficient is triggered when V_{AFt}/V_p^{max} and V_{Frie}/V_p^{max} reach 0.21 and 0.45, respectively. The effects of ettringite filling are more significant than that of Friedel's salt.

4.3. Competitive binding of chloride and sulfate ions

4.3.1. The influence of filling on the transport of sulfate and chloride ions

Without considering the influence of fluid movement in pore solution, the diffusion of ions is driven by the gradient of concentration. Chloride or sulfate ions penetrate to pore solution in concrete, releasing the competitive ions and form extra Friedel's salt or ettringite. The effects of filling and competitive binding on the concentration of sulfate and chloride ions are shown in Figs. 6 and 7, respectively. The results in Fig. 6 suggest that the filling effects are highly dependent on the SO_4^{2-}/Cl^- concentration ratio at boundary (The concentration of chloride was fixed at the concentration of chloride in seawater [46]). In contrast, the change of SO_4^{2-}

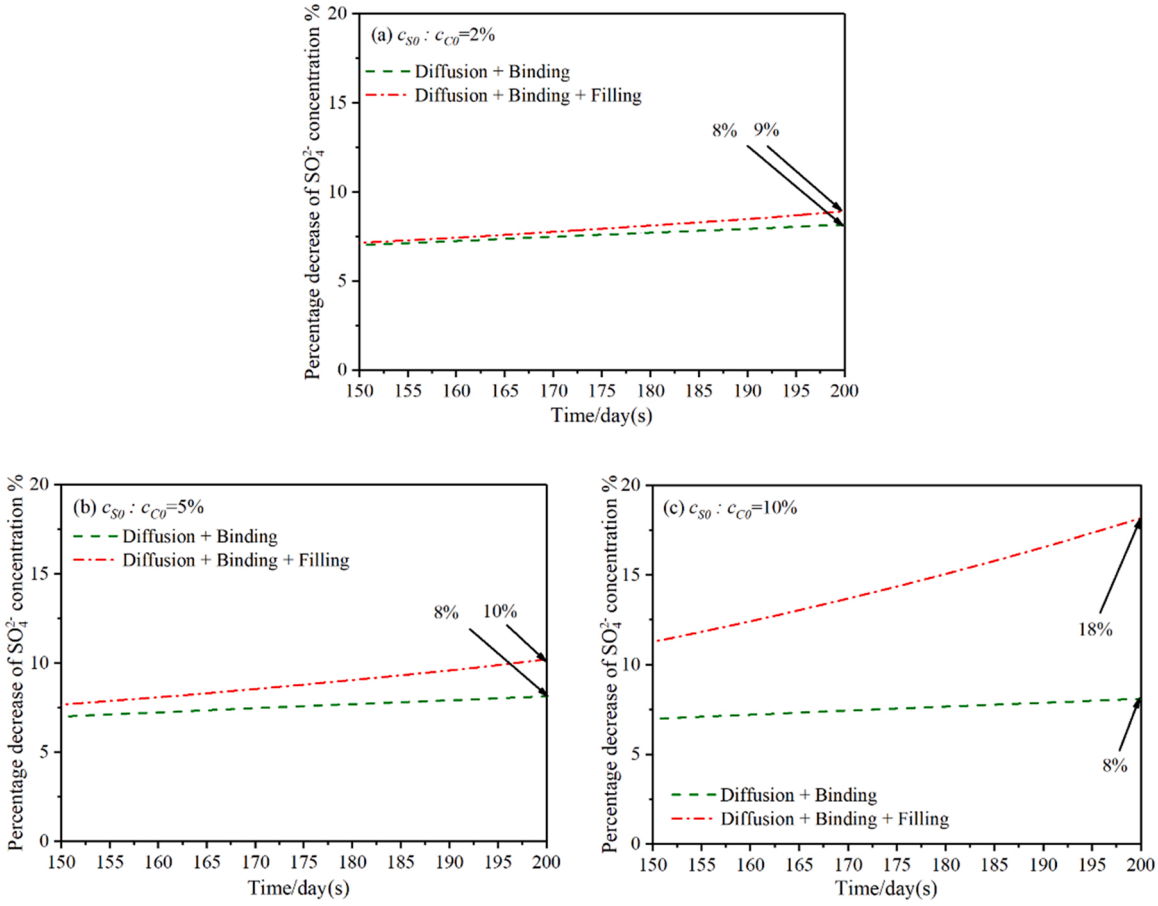

Fig. 6. Effects of binding and filling on the transport of SO_4^{2-} into concrete under different SO_4^{2-}/Cl^- ratios at the boundary (c_{C0} = 19. 162 g/kg).

concentration with increasing SO_4^{2-}/Cl^- ratio is not obvious when only diffusion and binding is considered in ion transportation. The percentage decrease of SO_4^{2-} and Cl^- concentration is 8% and 0.8%, respectively. A possible explanation for this phenomenon is that there are enough CA binding sites for both chloride and sulfate ions. Fig. 6 also shows that, after 200 days of penetration, the filling effects can reduce SO_4^{2-} concentration by more than 10% compared to the case without considering the filling effects. In contrast, the filling effects show limited influence on time-dependent decrease of Cl^- concentration (Fig. 7).

4.3.2. *The influence of CA binding sites on the transport of sulfate and chloride ions*

Fig. 8 show the influence of varied $c_{CA}/c_{CA\text{-}T}$ ratios on sulfate and chloride concentration (depth = 10 mm, t = 100 days). The results reveal that the concentration of free sulfate and chloride ions can significantly decrease when binding site concentration is high (*e.g.* $c_{CA}/c_{CA\text{-}T} > 1$), whereas under a low binding site concentration (*e.g.* $c_{CA}/c_{CA\text{-}T} < 0.1$), the change of binding site concentration has little influence on sulfate and chloride ion concentration due to the saturated binding sites. Factors influencing the binding involves cement type (*i.e.* the content of C_3A), cement replacement, cation, temperature, and water-binder ratio, etc [47], and most of the factors are essentially changing the number of effective binding sites.

4.4. *The influence of competitive binding on chloride-induced corrosion*

The free chloride uptake ratio (R_F) of 0.569 ± 0.117 might lead to the initiation of steel bar depassivation in concrete as shown in the available reports [48], and the value varies depending on many factors such as humidity, temperature and pitting potential and *etc.* Fig. 9(a) shows the change of free chloride uptake with time under chloride condition only. The model prediction shows that the initial corrosion time of concrete is around 8 years when the cover thickness of reinforcement bars is 65 mm. When concrete structures are immersed in a mixture of chloride and sulfate ions, the corrosion situation is different. The time-dependent normalized maximum strain under both chloride and sulfate condition is shown in Fig. 9(b). It is known that sulfate attack leads to the expansion of concrete and then cracking and spalling of the outermost layers, which in turn accelerates the ions transport significantly. Therefore, it is assumed that the corrosion initiates once the crack occurs when specimens are immersed in the mixed sulfate and chloride solution, *e.g.* shorten the initial corrosion time to 340 days when immersed in the combined chloride and sulfate solution.

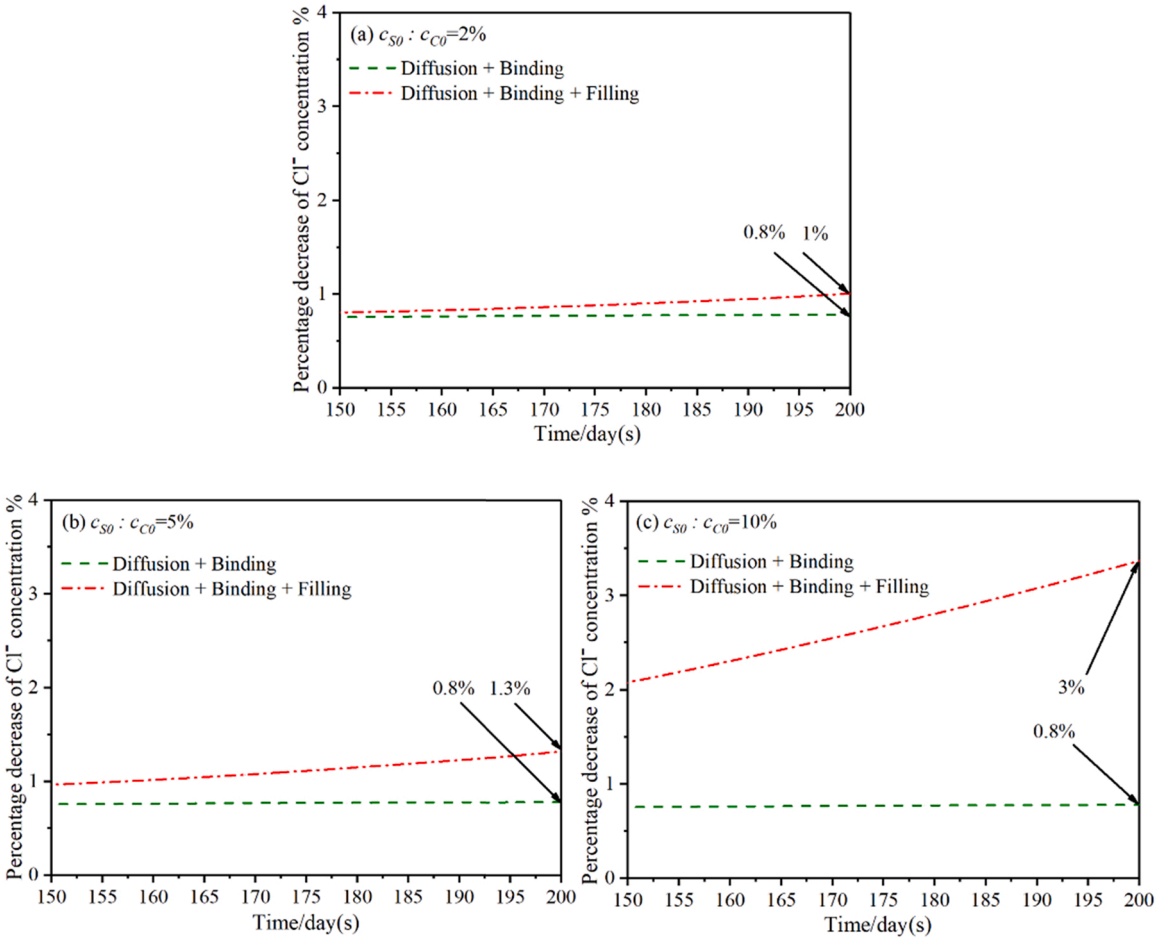

Fig. 7. Effects of binding and filling on the transport of Cl^- into concrete under different SO_4^{2-}/Cl^- ratios at the boundary (c_{C0} = 19. 162 g/kg).

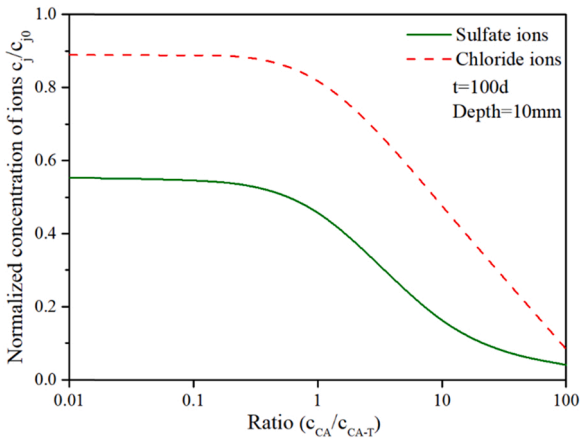

Fig. 8. Normalized concentration of ions in concrete immersed in seawater at various binding sites solution ($j = 1$ refers to Cl^- and $j = 2$ refers to SO_4^{2-}).

Fig. 10 shows the initial corrosion time of steel bars in concrete specimens under the combined sulfate and chloride solution with different SO_4^{2-}/Cl^- ratios at the boundary by fixing chloride concentration (c_{C0} = 19.162 g/kg in seawater [46]). It indicates that the increase in sulfate concentration can decrease the initial corrosion time of concrete. For example, the increase of SO_4^{2-}/Cl^- ratio from 2% to 10% could shorten the initial corrosion time from 878 days to 183 days. Therefore, even though sulfate ion accounts for only a small

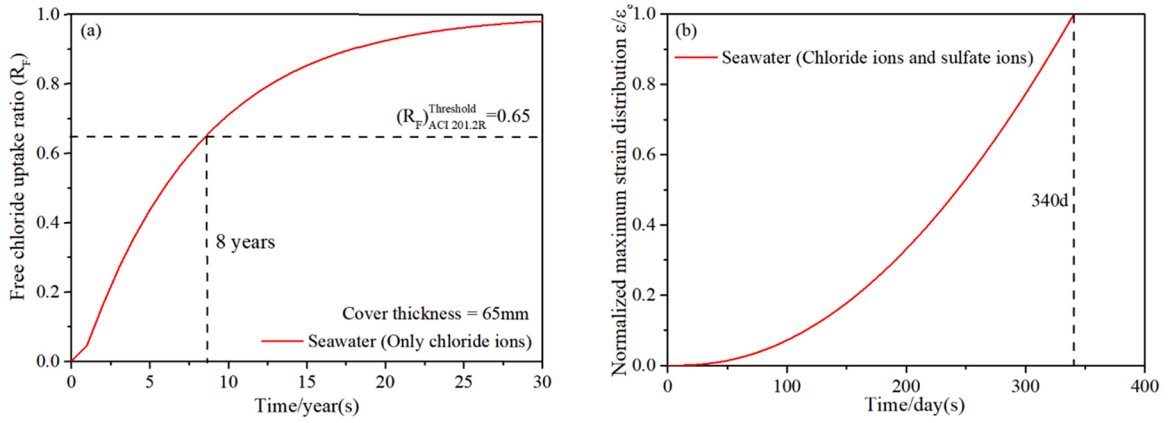

Fig. 9. Initial corrosion time of steel bars in concrete immersed in seawater (Cover thickness = 65 mm) (a) Exposed to chloride ions only, and (b) Exposed to both sulfate and chloride ions, $c_{C0} = 19.162$ g/kg, $c_{S0} = 2.68$ g/kg, ε_e refers to the maximum elastic strain of concrete.

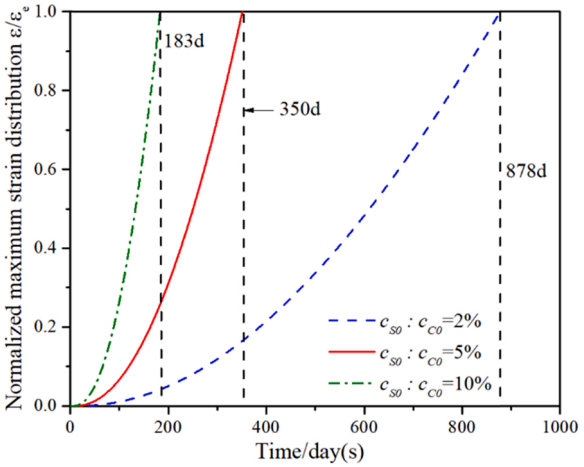

Fig. 10. Initial corrosion time of steel bars in concrete specimens under both sulfate and chloride attack with different SO_4^{2-}/Cl^- ratios (c_{C0} = 19.162 g/kg).

proportion in the corrosion environment, its destructive effect on chlorine ion or other ions cannot be ignored.

5. Conclusions

The role of reactive transport and competitive binding of sulfate and chloride ions in the deterioration of offshore concrete structures was investigated in the present study through developing a theoretical model in conjunction with experimental studies. The early stage before cracks initiation was studied and the following conclusions are reached:

- The transport of sulfate ions under different combinations of sulfate and chloride concentrations with time can be modelled by using the parameters of K and m (*i.e.* $K_{a1} = 0.21$, $K_{a2} = 0.45$, $m_1 = 2$ and $m_2 = 7$) obtained through calibrating experimental data. The decrease of diffusion coefficients of ions during early period is due to the filling effects of deterioration products precipitated in concrete pores.
- At the initial stage (*i.e.* first 20 days), there is a significant increase in the concentration of sulfate ions, and the increasement rate remains stable with time.
- There is a considerably decrease in the diffusion coefficient of ions on account of the filling of reaction product, and the effects of ettringite filling are more significant ($V_{AFt}/V_p^{max} = 0.21$) than that of Friedel's salt ($V_{Frie}/V_p^{max} = 0.45$). In addition, the filling effects can decrease sulfate concentration in concrete by more than 10% at 200 days whereas filling has limited influence on chloride concentration.

- The concentration of free sulfate and chloride ions can significantly decrease with the increase of binding sites. However, under a low binding site concentration (*e.g.* $c_{CA}/c_{CA\text{-}T} < 0.1$), the change of binding site has little influence on sulfate and chloride ion concentration due to the saturation of binding sites.
- The transport of sulfate ions into concrete could shorten the initial time of corrosion induced by chloride ions, especially when SO_4^{2-}/Cl^- ratio (c_{s0}/c_{c0}) is high. For example, the increase of c_{s0}/c_{c0} from 2% to 10% could shorten the initial corrosion time from 878 days to 183 days.

Declaration of Competing Interest

The authors declare that they have no known competing financial interests or personal relationships that could have appeared to influence the work reported in this paper.

Data availability statement

The data that support the findings of this study are available on request from the corresponding author.

Acknowledgments

The authors acknowledge the financial support provided by Shanghai Pujiang Program (21PJ1423700), the National Natural Science Foundation of China (51978505, 51608382), Shanghai Rising-Star Program (20QC1400600) and Science and Technology R&D Programs of China Railway Construction Corporation Limited (2019-C15).

References

[1] O.T. de Rincón, M. Sánchez, V. Millano, R. Fernández, E. de Partidas, C. Andrade, I. Martínez, M. Castellote, M. Barboza, F. Irassar, Effect of the marine environment on reinforced concrete durability in Iberoamerican countries: DURACON project/CYTED, Corros. Sci. 49 (7) (2007) 2832–2843, https://doi.org/10.1016/j.corsci.2007.02.009.
[2] D. Li, L.Y. Li, X. Wang, Chloride diffusion model for concrete in marine environment with considering binding effect, Mar. Struct. 66 (JUL.) (2019) 44–51, https://doi.org/10.1016/j.marstruc.2019.03.004.
[3] P.K. Mehta, Mechanism of sulfate attack on portland cement concrete — Another look, Cem. Concr. Res. 13 (3) (1983) 401–406, https://doi.org/10.1016/0008-8846(83)90040-6.
[4] G. Rajasekaran, Sulphate attack and ettringite formation in the lime and cement stabilized marine clays, Ocean Eng. 32 (8) (2005) 1133–1159, https://doi.org/10.1016/j.oceaneng.2004.08.012.
[5] S. Real, J.A. Bogas, Chloride ingress into structural lightweight aggregate concrete in real marine environment, Mar. Struct. 61 (SEP.) (2018) 170–187, https://doi.org/10.1016/j.marstruc.2018.05.008.
[6] F. Tittarelli, A. Mobili, C. Giosuè, A. Belli, T. Bellezze, Corrosion behaviour of bare and galvanized steel in geopolymer and Ordinary Portland Cement based mortars with the same strength class exposed to chlorides, Corros. Sci. 134 (2018) 64–77, https://doi.org/10.1016/j.corsci.2018.02.014.
[7] H.S. Al-Alaily, A.A.A. Hassan, Time-dependence of chloride diffusion for concrete containing metakaolin, J. Build. Eng. 7 (2016) 159–169, https://doi.org/10.1016/j.jobe.2016.06.003.
[8] M.U. Khan, S. Ahmad, H.J. Al-Gahtani, Chloride-induced corrosion of steel in concrete: an overview on chloride diffusion and prediction of corrosion initiation time, Int J. Corros. 2017 (2017), https://doi.org/10.1155/2017/5819202.
[9] S. Muthulingam, B.N. Rao, Consistent models for estimating chloride ingress parameters in fly ash concrete, J. Build. Eng. 3 (2015) 24–38, https://doi.org/10.1016/j.jobe.2015.04.009.
[10] A.R. Al-Rabiah, Rasheeduzzafar, R. Baggott, Durability requirements for reinforced concrete construction in aggressive marine environments, Mar. Struct. 3 (4) (1990) 285–300, https://doi.org/10.1016/0951-8339(90)90013-H.
[11] L. Bertolini, M. Gastaldi, M. Pedeferri, E. Redaelli, Prevention of steel corrosion in concrete exposed to seawater with submerged sacrificial anodes, Corros. Sci. 44 (7) (2002) 1497–1513, https://doi.org/10.1016/S0010-938X(01)00168-8.
[12] A.M. Ragab, M.A. Elgammal, O.A. Hodhod, T.E. Ahmed, Evaluation of field concrete deterioration under real conditions of seawater attack, Constr. Build. Mater. 119 (2016) 130–144, https://doi.org/10.1016/j.conbuildmat.2016.05.014.
[13] K. Sotiriadis, E. Nikolopoulou, S. Tsivilis, Sulfate resistance of limestone cement concrete exposed to combined chloride and sulfate environment at low temperature, Cem. Concr. Compos. 34 (8) (2012) 903–910, https://doi.org/10.1016/j.cemconcomp.2012.05.006.
[14] M. Maes, N. De Belie, Resistance of concrete and mortar against combined attack of chloride and sodium sulphate, Cem. Concr. Compos. 53 (2014) 59–72, https://doi.org/10.1016/j.cemconcomp.2014.06.013.
[15] M. Zhang, J. Chen, Y. Lv, D. Wang, J. Ye, Study on the expansion of concrete under attack of sulfate and sulfate–chloride ions, Constr. Build. Mater. 39 (2013) 26–32, https://doi.org/10.1016/j.conbuildmat.2012.05.003.
[16] D.A. Wiesenburg, B.J. Little, A synopsis of the chemical/physical properties of seawater, Appl. Ocean Phys. Eng. (1988), https://doi.org/10.1016/0029-8018(88)90005-4.
[17] T. Luping, J. Gulikers, On the mathematics of time-dependent apparent chloride diffusion coefficient in concrete, Cem. Concr. Res. 37 (4) (2007) 589–595, https://doi.org/10.1016/j.cemconres.2007.01.006.
[18] T. Senga Kiesse, S. Bonnet, O. Amiri, A. Ventura, Analysis of corrosion risk due to chloride diffusion for concrete structures in marine environment, Mar. Struct. 73 (2020), 102804, https://doi.org/10.1016/j.marstruc.2020.102804.
[19] M. Satyanarayana, Y. Kalpana, V. Himabindu, K. Kumar, Novel molecular approach using triazine inhibitor to control corrosion and limit chloride ion penetration in steel reinforced concrete, Corros. Eng. Sci. Tech. 47 (1) (2012) 38–44, https://doi.org/10/1179/1743278211Y.0000000015.
[20] S. Hartshorn, J. Sharp, R. Swamy, Thaumasite formation in Portland-limestone cement pastes, Cem. Concr. Res. 29 (8) (1999) 1331–1340, https://doi.org/10.1016/S00088846(99)00100-3.
[21] T. Schmidt, B. Lothenbach, M. Romer, J. Neuenschwander, K. Scrivener, Physical and microstructural aspects of sulfate attack on ordinary and limestone blended Portland cements, Cem. Concr. Res. 39 (12) (2009) 1111–1121, https://doi.org/10.1016/j.cemconres.2009.08.005.
[22] De Weerdt, K. and M. Geiker.: Changes in the phase assemblage of concrete exposed to seawater—case study. Proceeding of the proceedings of the international congress on durability of concrete (ICDC 2012), NTNU Trondheim, Trondheim.(2012).
[23] R. Kaminskas, I. Barauskas, Influence of pozzolana on sulfate attack of cement stone affected by chloride ions, Mater. Struct. 47 (11) (2014) 1901–1910, https://doi.org/10.1617/s11527-013-0159-5.

[24] X. Ouyang, L. Wang, S. Xu, Y. Ma, G. Ye, Surface characterization of carbonated recycled concrete fines and its effect on the rheology, hydration and strength development of cement paste, Cem. Concr. Compos. 114 (2020), 103809, https://doi.org/10.1016/j.cemconcomp.2020.103809.
[25] K. Wu, Y. Hu, L. Zhang, L. Xu, Z. Yang, Promoting the sustainable fabrication of bricks from municipal sewage sludge through modifying calcination: Microstructure and performance characterization, Constr. Build. Mater. 324 (2022), 126401, https://doi.org/10.1016/j.conbuildmat.2022.126401.
[26] A. Abdalkader, C. Lynsdale, J. Cripps, The effect of chloride on performance of cement mortars subjected to sulfate exposure at low temperature, Constr. Build. Mater. 78 (2015) 102–111, https://doi.org/10.1016/j.conbuildmat.2014.12.006.
[27] O.S.B. Al-Amoudi, M. Maslehuddin, The effect of chloride and sulfate ions on reinforcement corrosion, Cem. Concr. Res. 23 (1) (1993) 139–146, https://doi.org/10.1016/0008-8846(93)90144-X.
[28] X. Ouyang, D.A. Koleva, G. Ye, K. van Breugel, Understanding the adhesion mechanisms between CSH and fillers, Cem. Concr. Res 100 (2017) 275–283, https://doi.org/10.1016/j.cemconres.2017.07.006.
[29] Z. Wang, Y. Chen, L. Xu, Z. Zhu, Y. Zhou, F. Pan, K. Wu, Insight into the local C-S-H structure and its evolution mechanism controlled by curing regime and Ca/Si ratio, Constr. Build. Mater. 333 (2022), 127388, https://doi.org/10.1016/j.conbuildmat.2022.127388.
[30] D.R. Lide, CRC handbook of chemistry and physics, CRC press, 2004.
[31] S. Ekolu, M. Thomas, R. Hooton, Pessimum effect of externally applied chlorides on expansion due to delayed ettringite formation: proposed mechanism, Cem. Concr. Res. 36 (4) (2006) 688–696, https://doi.org/10.1016/j.cemconres.2005.11.020.
[32] K. Wu, H. Han, H. Li, B. Dong, T. Liu, G. De Schutter, Experimental study on concurrent factors influencing the ITZ effect on mass transport in concrete, Cem. Concr. Compos. 123 (2021), 104215, https://doi.org/10.1016/j.cemconcomp.2021.104215.
[33] L. Zhang, B.S. Gardiner, D.W. Smith, P. Pivonka, A.J. Grodzinsky, IGF uptake with competitive binding in articular cartilage, J. Biol. Syst. 16 (2) (2008) 175–195, https://doi.org/10.1142/S0218339008002575.
[34] D. Sun, K. Wu, H. Shi, S. Miramini, L. Zhang, Deformation behaviour of concrete materials under the sulfate attack, Constr. Build. Mater. 210 (2019) 232–241, https://doi.org/10.1016/j.conbuildmat.2019.03.050.
[35] Jk Chen, Mq Jiang, J. Zhu, Damage evolution in cement mortar due to erosion of sulphate, Corros. Sci. 50 (9) (2008) 2478–2483, https://doi.org/10.1016/j.corsci.2008.05.021.
[36] W. Chalee, C. Jaturapitakkul, P. Chindaprasirt, Predicting the chloride penetration of fly ash concrete in seawater, Mar. Struct. 22 (3) (2009) 341–353, https://doi.org/10.1016/j.marstruc.2008.12.001.
[37] S. Muthulingam, B. Rao, Non-uniform time-to-corrosion initiation in steel reinforced concrete under chloride environment, Corros. Sci. 82 (2014) 304–315, https://doi.org/10.1016/j.corsci.2014.01.023.
[38] C.B. Shin, E.K. Kim, Modeling of chloride ion ingress in coastal concrete, Cem. Concr. Res. 32 (5) (2002) 757–762, https://doi.org/10.1016/S0008-8846(01)00756-6.
[39] D. Sun, K. Wu, H. Shi, L. Zhang, L. Zhang, Effect of interfacial transition zone on the transport of sulfate ions in concrete, Constr. Build. Mater. 192 (2018) 28–37, https://doi.org/10.1016/j.conbuildmat.2018.10.140.
[40] K. Nakarai, T. Ishida, K. Maekawa, Modeling of calcium leaching from cement hydrates coupled with micro-pore formation, J. Adv. Concr. Technol. 4 (3) (2006) 395–407, https://doi.org/10.3151/jact.4.395.
[41] P. Gospodinov, R. Kazandjiev, M. Mironova, The effect of sulfate ion diffusion on the structure of cement stone, Cem. Concr. Compos. 18 (6) (1996) 401–407, https://doi.org/10.1016/S0958-9465(96)00032-7.
[42] V.G. Papadakis, M.N. Fardis, C.G. Vayenas, Physicochemical processes and mathematical modeling of concrete chlorination, Chem. Eng. Sci. 51 (4) (1996) 505–513, https://doi.org/10.1016/0009-2509(95)00318-5.
[43] U. Birnin-Yauri, F. Glasser, Friedel's salt, $Ca_2Al(OH)_6$ (Cl, OH)·$2H_2O$: its solid solutions and their role in chloride binding, Cem. Concr. Res. 28 (12) (1998) 1713–1723, https://doi.org/10.1016/S0008-8846(98)00162-8.
[44] A. Suryavanshi, J. Scantlebury, S. Lyon, Mechanism of Friedel's salt formation in cements rich in tri-calcium aluminate, Cem. Concr. Res. 26 (5) (1996) 717–727, https://doi.org/10.1016/S0008-8846(96)85009-5.
[45] C. Sun, J. Chen, J. Zhu, M. Zhang, J. Ye, A new diffusion model of sulfate ions in concrete, Constr. Build. Mater. 39 (2013) 39–45, https://doi.org/10.1016/j.conbuildmat.2012.05.022.
[46] F.J. Millero, R. Feistel, D.G. Wright, T.J. McDougall, The composition of standard seawater and the definition of the reference-composition salinity scale, Deep Sea Res (I: Oceano Res Pap.) 55 (1) (2008) 50–72, https://doi.org/10.1016/j.dsr.2007.10.001.
[47] L. Tang, Chloride transport in concrete-measurement and prediction (Doctor Thesis), Chalmers University of Technology, Sweden, 1996.
[48] D. Izquierdo, C. Alonso, C. Andrade, M. Castellote, Potentiostatic determination of chloride threshold values for rebar depassivation: experimental and statistical study, in: Electrochimica Acta, 49, 2004, pp. 2731–2739, https://doi.org/10.1016/j.electacta.2004.01.034.